Highlight Review

Recent Advances in Phosphorescent Pt(II) Complexes Featuring Metallophilic Interactions: Properties and Applications

Alessandro Aliprandi,[1] Damiano Genovese,[2] Matteo Mauro,[*1,3] and Luisa De Cola[1,2]

[1]Laboratoire de Chimie et des Biomatériaux Supramoléculaires, ISIS and icFRC,
Université de Strasbourg and CNRS, 8 allée Gaspard Monge, 67000 Strasbourg, France
[2]Karlsruher Institut für Technologie (KIT) Institut für Nanotechnologie,
Hermann-von-Helmholtz-Platz 1 D - 76344 Eggenstein-Leopoldshafen, Germany
[3]University of Strasbourg Institute for Advanced Study (USIAS),
5 allée du Général Rouvillois, 67083 Strasbourg, France

(E-mail: mauro@unistra.fr)

Luisa De Cola is since September 2013 Professor at the University of Strasbourg (I.S.I.S.) as chair of Supramolecular and Bio-Material Chemistry, and part time scientist at the INT-KIT, Karlsruhe, Germany. She was born in Messina, Italy, where she studied chemistry. After a post-doc in USA she moved back to Italy and in 1990 she was appointed Assistant Professor at the University of Bologna (Prof. V. Balzani group). In 1998 she moved as Full Professor to the University of Amsterdam, The Netherlands. In 2004 she accepted a call from Germany at the University of Münster as full professor in chemistry and physics. She has received several awards, the most recent being the ERC advanced grant (2009), the IUPAC award as one of the Distinguished Women in Chemistry and Chemical Engineering (2011), the Gutenberg chair award (2012), and the International Prize for Chemistry "Prof. Luigi Tartufari" from Accademia dei Lincei (2014). She was elected as member of the Academia Europeae in 2012 and, in 2014, member of the German National Academy of Sciences Leopoldina. In 2014 she has been Nominated "Chevalier de la Légion d'Honneur" by the President of the French Republic, François Hollande. In 2015 she received the Catalán-Sabatier-Award. She has published 300 papers, 30 patents and she has a H index of 58 (>11400 citations). Her main interests are luminescent molecules and their assemblies for the creation of novel materials and nanostructures for bio-applications.

Dr. Matteo Mauro obtained his B.Sc. *cum laude* in Chemistry at the University of Bari (Italy) in 2004 and his M.Sc. (2006) and Ph.D. (2009) degree in Chemical Sciences at the University of Milano (Italy). After postdoctoral experiences at the University of Münster, Germany, since 2012 he has been appointed as Assistant Professor and he received his Habilitation (HDR) in 2014 at the University of Strasbourg, Institut de Science et d'Ingénierie Supramoléculaires (I.S.I.S.), in the group of Prof. L. De Cola. To date, he has been awarded the Eni Award "debut research prize" (2010), Alexander von Humboldt fellowship (2011), and University of Strasbourg Institute for Advanced Studies (USIAS) fellowship (2013). His current research focuses on self-assembling (electro)-luminescent transition-metal complexes and their application as well as light-driven smart materials for soft robotics.

Alessandro Aliprandi received his M.Sc. degree in Chemistry from the University of Ferrara in 2010 under the supervision of Prof. C. A. Bignozzi. After a one year fellowship in the same group, he joined Prof. Luisa De Cola's group as a Ph.D. candidate at the University of Strasbourg, at the Institut de Science et d'Ingénierie Supramoléculaires (I.S.I.S.). His research focuses on self-assembly of luminescent transition-metal complexes and their application in bio-imaging.

Dr. Damiano Genovese obtained his Ph.D. in Chemistry at University of Bologna in 2011, under the supervision of Prof. Luca Prodi. He was a visiting student at the Ecole Normale Superieure (France) and at the Harvard University (USA), and he carried out postdoctoral research in Bologna until 2013. He was awarded the ENI prize 2013 for his "Debut in Research", and then moved at the Karlsruhe Institute of Technology (Germany) in the research group of Prof. Luisa De Cola, where he is currently an Alexander von Humboldt postdoctoral fellow.

Abstract

Supramolecular weak interactions can be used for preparing functional self-assembled architectures by powerful *bottom-up* approaches. In particular, when closed-shell metallophilic and π–π interactions between adjacent transition-metal complexes are established, profound changes in compounds' properties are obtained and novel features often achieved. In this Review, the most recent advances in the field of luminescent platinum(II) complexes aggregating through Pt–Pt interactions are highlighted and their potential application in different fields presented and discussed.

Introduction

Luminescent coordination compounds able to efficiently emit from an excited state with formally triplet character have been a matter of intense research in the last few decades.[1–7] Such complexes, which are able to radiatively relax from an excited state back to the ground state through formally spin-forbidden transitions (*phosphorescence*), display photochemical and photophysical features different from classical organic fluorophores, making them peculiar and attractive.

Nowadays, widespread interest towards phosphorescent molecular compounds is powered by their potential and real-market application in areas which span from optoelectronics,[8–10] solar-energy conversion,[11,12] sensing,[13] bioimaging,[14–16] and photocatalysis.[17]

In particular, it is possible to prepare luminescent complexes with great photoluminescence quantum yield (PLQY) up to nearly unity and radiative lifetime in the few microseconds regime both in fluid solution and in condensed phases by proper choice of the coordination environment. Furthermore, the electronic properties of both metal center and substituents onto the coordinated ligands allow easy addressable modulation of both redox and emission properties with luminescence colors adjustable over the entire visible spectrum and beyond.[2,8,9]

Also, for derivatives based on the second and third row of the transition metal block, such as d^6 Ir(III), Ru(II), Os(II), and Re(I), as well as d^8 Pt(II) and Au(III),[18,19] and d^{10} Au(I),[20,21] the sizeable spin–orbit coupling effect induced by the heavy atom promotes fast and efficient intersystem crossing process between singlet- and triplet-manifold electronic states, yielding triplet excited states with radiative rate constants (k_r) capable of efficiently competing with the radiationless deactivation pathways (Σk_{nr}).

While metal atoms with d^6 valence shell electronic configuration typically show octahedral arrangement providing an essentially spherical shape to the molecule; d^8 counterparts, such as Pt(II) derivatives, display a (distorted) square-planar molecular geometry around the metal center. As it will be hereafter discussed, such difference induces profound variations in their photophysical properties of both their ground and excited states due to the tendency to give face-to-face interaction. In particular, the presence of the filled d_{z^2} orbital normal to the molecular plane is, in some cases, responsible for the establishment of weak dispersion intermolecular interactions as consequence of the closed-shell metal⋯metal electronic overlap, called metallophilic interaction.[22,23]

To date, an impressive number of papers report on the synthetic pathways and characterization of transition-metal complexes showing metallophilic interactions, with particular focus on the solid-state polymorphism.[24–26]

Thus, the aim of the present review is to highlight those contributions from either our or other research groups in which the role of the metallophilic interactions is to promote supramolecular organization from zero-dimensional (0D) architectures up to three-dimensional (3D) networks that give rise to attractive changes of the properties, and/or in which the molecular systems have been ultimately used as materials for applicative purposes.

Hence, due to space constraints, we will hereafter limit our attention to selected and most recent developments and contributions in such growing interesting area dealing with luminescent platinum(II) derivatives. Nonetheless, the review is far from being exhaustive and the readers will be each time invited to refer elsewhere when the corresponding subject has been already reviewed.

Photophysics of Pt(II) Complexes: Background

Although a detailed description of the photochemistry and photophysics of platinum complexes is beyond the scope of the present review, we would like to recall some basics aspects of the photophysical features that are typical of this class of compounds to better follow the following discussion; interested readers are kindly invited to refer to other reviews and books for a more exhaustive discussion.[27]

As far as transition-metal complexes are concerned, the presence of the metal atom induces admixing of the metal d orbitals with the counterparts located on the conjugated ligands possessing π-character. This mixing yields electronic transitions between filled and empty, i.e. virtual, orbitals with different character that can be sorted depending on the nature and location of the involved orbitals. Thus, optical electronic transition with either ligand-centered (LC), metal-centered (MC), metal-to-ligand (MLCT), ligand-to-metal (LMCT), and ligand-to-ligand (LLCT) charge transfer is possible as schematically displayed in Figure 1.

As far as transitions with LC nature are concerned, during optical process reorganization of the electron density take place between bonding and antibonding orbitals with either n or π character mainly localized on the ligands; whilst, processes with MC processes involve orbital with d character located on the metal atom.

The concomitant presence of both metal and conjugated aromatic ligands allows the possibility to have charge transfer transitions with either MLCT or LMCT character, in which the reorganization of the electron density can be at first-approximation described as d → π* or π → d*, respectively. On the other hand, when electron density reorganization take place between different ligands (π → π*) the transition is called ligand-to-ligand charge transfer, namely LLCT.

It is also worth to notice that coordination of π-conjugated and strong ligand-field moieties, such as σ-donor and cyclometalating ligands, raises the thermally-accessible quenching MC excited state to higher energies with respect to LC and MLCT states, thus yielding complexes with greater emission properties. Triplet excited states with MLCT, ^{3}MLCT, character are indeed characterized by much larger k_r (in the order of 10^4–
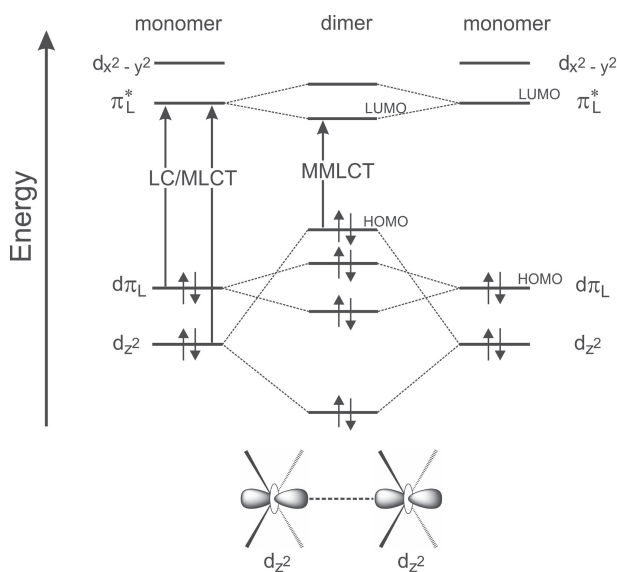
Figure 1. Simplified molecular orbital (MO) diagram of two interacting platinum(II) complexes at their ground state. The diagram highlights the intermolecular metallophilic interaction through the $d_{z^2} \cdots d_{z^2}$ orbitals overlap and the consequent influence on the MO energy levels.

$10^5 \, \text{s}^{-1}$) than ^{3}LC and MC states, also owing to the contribution of the heavy metal orbitals and SOC effect.

The square-planar geometry of platinum(II) complexes along with the presence of filled d_{z^2} orbitals, which are oriented normal to the molecular plane, make such complexes very different from other luminescent compounds. The flat geometry allows indeed efficient face-to-face intermolecular interactions at either the ground or the excited state. In the latter case, either excimer or exciplex formation is possible, whether the interaction is between the same or different molecules, respectively.

In the former case, axial interaction could take place when the intermolecular distance is in the range 3.0–3.5 Å, which typically involves π–π stacking and metal⋯metal ($d_{z^2} \cdots d_{z^2}$) orbital overlap. The establishment of this metallophilic interaction is accompanied by profound changes with respect to the noninteracting molecules that imply richer and unique electronic, spectroscopic, and redox properties. Hence, the close proximity and interaction of the platinum complexes induces a change of the nature of the highest occupied MO as consequence of the destabilization of the d_{z^2} orbitals when compared to the noninteracting molecules, giving rise to the possibility of transitions with metal-metal-to-ligand charge transfer (MMLCT) nature, dσ*(metal) → π*(ligand), that is shifted to lower energy than either LC or MLCT transition of the parental molecules (Figure 1).

From Molecules to 3D Architectures

Supramolecular chemistry plays a key role in a number of research fields, such as chemical and material science, as well as biology, allowing the precise assembly of randomly oriented molecules into highly ordered supramolecular structures by means of delicate balance of weak noncovalent interactions. Deep understanding of such interactions that govern supra-

molecular assemblies and determine the different hierarchies of organization is of paramount importance, as these interactions would in turn affect the properties of the final system.[28,29] The self-organization of phosphorescent platinum(II) complexes containing π-conjugated ligands through Pt⋯Pt and/or ligand–ligand interactions has been employed in the last decades as an efficient *bottom-up* approach towards preparation and development of novel molecular materials from the molecular up to micrometer scale.[30–34] Furthermore, the anisotropic growth of ordered supramolecular structures often observed in such systems suggests that molecular propagation is faster along the axis of the Pt⋯Pt interaction than in the lateral directions.[35,36] Nevertheless, only very recently a cooperative growth mechanism was demonstrated for the self-assembly of Pt(II) complexes,[37,38] which can be considered as a milestone to find reasonable explanation for the formation of highly organized aggregates with well-defined size, shapes, and properties. Due the weak and noncovalent nature of the Pt⋯Pt interaction, the so-formed self-assembled architectures are generally very much affected by changes in the microenvironment such as temperature, solvent compositions, and counter ions. Furthermore, when stimuli-responsive groups are incorporated into these building blocks, the assembling and disassembling behavior can be controlled by application of external stimuli like pH, temperature, redox, and light, amongst all.[39,40]

Distinctive spectroscopic properties, such as both lower-energy absorption and/or emission bands, have often been observed and considered as a fingerprint of the establishment of Pt⋯Pt interactions. Change of such properties can be hence used to probe dynamic transformation of the supramolecular assemblies.[7,10,36] As a result, a rich variety of supramolecular functional architectures has been reported which range from pseudo-0D structures such as micelles, to 1D arrays, to 2D layers, and up to 3D networks. As consequence of their square-planar molecular geometry, the most commonly observed self-assembly form is certainly fibrils (1D) that often tend to bundle into entangled 3D networks leading, in some cases, to the formation of supramolecular gels.[32,41,42] In this respect, terpyridine σ-alkynyl Pt(II) complexes have received considerable attention in recent years due to their photoluminescence properties.[43] An example of how color changes can be used to probe the self-assembly process has been reported by Chan et al.[44] Interestingly, such compounds are not only sensitive to the changes in the microenvironment, upon variations of solvent compositions, counter ions, and pH, but positively charged alkynylplatinum(II) terpyridyl complexes can interact with several (bio-)polymers carrying multiple negatively charged functional groups[45] or biologically relevant biomolecules, such as citrate, thus allowing the monitoring of enzymatic activities.[46] Also oligonucleotides[30] were found to interact with such class of Pt(II) complexes, resulting into a stabilization of the helical conformation through Pt⋯Pt and π⋯π interactions as revealed by significant enhancement of circular dichroism (CD) signal (Figure 2).

Among all the reported alkynylplatinum(II) complexes, those bearing an amphiphilic anionic bzimpy moiety as terdentate ligand, where bzimpy is 2,6-bis(*N*-alkylbenzimidazol-2′-yl)pyridine (Chart 1), have shown very interesting properties in terms of morphological transformation associated with spectroscopic changes both in terms of photoluminescence and electronic absorption.[47] At high water content, pseudo-0D
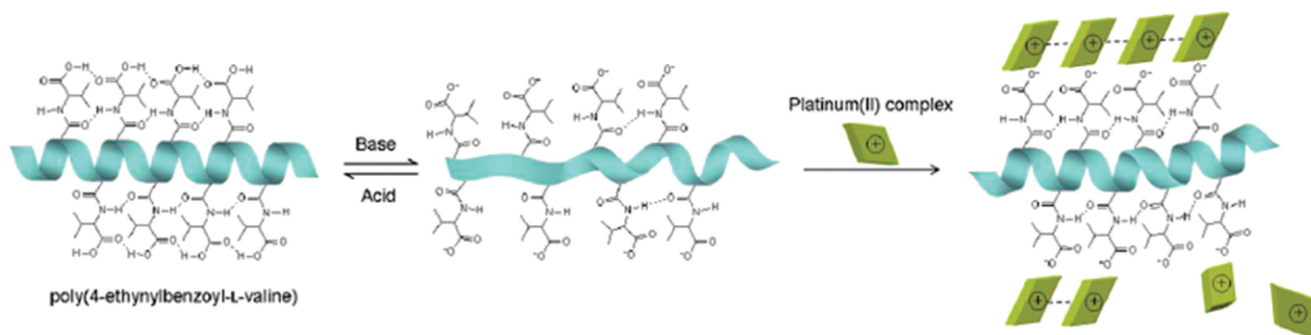
Figure 2. Scheme of the proposed chain helicity modulation of poly(4-ethynylbenzoly-L-valine) upon pH adjustment and upon interaction with a cationic platinum(II) complex. Adapted with permission from ref 43. Copyright (2011). American Chemical Society.
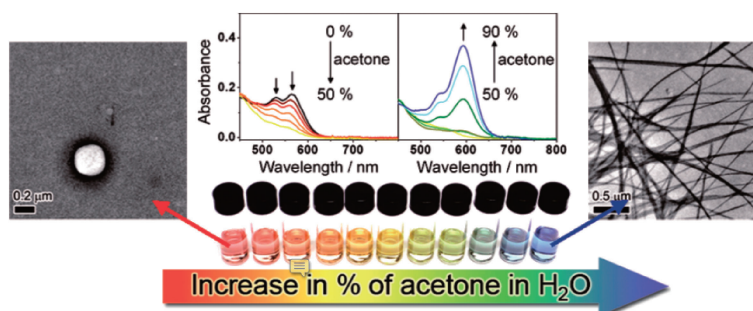
Figure 3. Correlation of the morphological with the spectroscopic properties obtained by varying the solvent composition for solution of complex **1a**. Adapted with permission from ref 47. Copyright (2011). American Chemical Society.

micellar structures have been observed, characterized by a broad featureless emission band ($\lambda_{em} = 675$–683 nm), attributed to a ^{3}MMLCT band due to ground-state Pt···Pt interactions. Interestingly, upon the addition of acetone to the aqueous solution of compound **1a**, the color of the solution changed from red to yellow to blue moving from 100% water to 1:1 and finally 9:1 acetone:water, respectively, as shown in Figure 3. Such spectroscopic changes were attributed to variation of the low-lying ^{1}MMLCT absorption bands.

In particular, the authors attributed the drop of the absorption bands at 532 and 564 nm for the red solution upon increasing the acetone content (pure water → 1:1 acetone:water) as indication of a partial disaggregation process with disruption of Pt···Pt and π–π interactions. At acetone concentration above 50%, formation of a new ^{1}MMLCT absorption bands at even lower energy was observed attributable to a second aggregated form with stronger Pt···Pt and π–π interactions. Interestingly, the formation of such second aggregates is affected by the ancillary ligand, where presence of a bulky trimethylsilyl group (**1b**) completely inhibited aggregation processes. As demonstrated by scanning electron microscopy (SEM) and transmission electron microscopy (TEM) images, the change of the spectroscopic properties for **1a** was accompanied by a neat variation of the morphological features of the aggregates in aqueous solutions from vesicular, at high water content, to long nanofibers at higher acetone content. It is likely that, in water, the charged sulfonate groups would point toward solvent molecules; while, the hydrophobic Pt(bzimpy) moieties would be forced to pack together through Pt···Pt and π–π stacking interactions in order to

avoid unfavorable contact with water, forming the bilayered structures of the vesicles. Upon addition of acetone, expected to well solvate Pt(bzimpy) moieties, the complex molecules would be better dispersed, resulting in the drop of the ^{1}MMLCT absorption band. Finally, as the acetone content is further increased, the sulfonate groups are no longer well solvated by the organic solvent; thus, the sulfonate ionic heads would start to aggregate and pull the complexes into close proximity, leading to their aggregation into nanofibers or nanorods.

In a more systematic study, the same group[48] reported on how the alkynyl functionalization, in particular, the alkyl chain lengths (complexes **2a–2g** in Chart 1) affects the self-assembly process in terms of both morphologic and spectroscopic properties.

Interestingly, in the absence of alkyl chain (**2a–2c**) the Pt(II) complexes gave similar structureless emission bands in the far-red region in aqueous media originating from ^{3}MMLCT excited state and associated with sheet-like structures (Figure 4). Increase of alkyl chain length to C7 (**2d**) induced a hypsochromic shift of the photoluminescence accompanied by appearance of vibronic structure. Upon further increase of chain length to C12 (**2e**), a gradual bathochromic shift of the emission maximum was observed and ascribed to the formation of fibrous nanostructures. The different morphology was rationalized in terms of the packing parameter (*P*), which correlates molecular structure with shape of amphiphiles and help to define molecular geometric criteria needed to pack molecules in a defined shape.

The incorporation of neutral triethylene glycol units into platinum(II) bzimpy scaffold, complex **3** in Chart 1, led to an

Chart 1. Chemical structures of the luminescent platinum(II) complexes used for the preparation of supramolecular architectures and herein reviewed.

unusual thermoresponsive behavior as demonstrated by temperature-dependent UV–visible absorption studies and heating–cooling cycles (Figure 5).[49]

The observed enhancement of the ¹MMLCT absorption and ³MMLCT emission band at higher temperature is contradictory to the commonly observed findings, i.e. that Pt⋯Pt interactions would usually be disrupted at elevated temperatures due to the molecular dissolution of the complex. Such finding along with electron microscopy analysis pointed towards formation of distinct assemblies at lower and higher temperature, namely micellar vs. bilayered structure, respectively.

Figure 4. (a) Normalized emission spectra of complex **2a**–**2g** in aqueous solution at concentration of 10^{-5} M; b) relationship between the packing parameter and the morphology of the self-assembled material. Adapted from ref 48 with permission of The Royal Society of Chemistry.
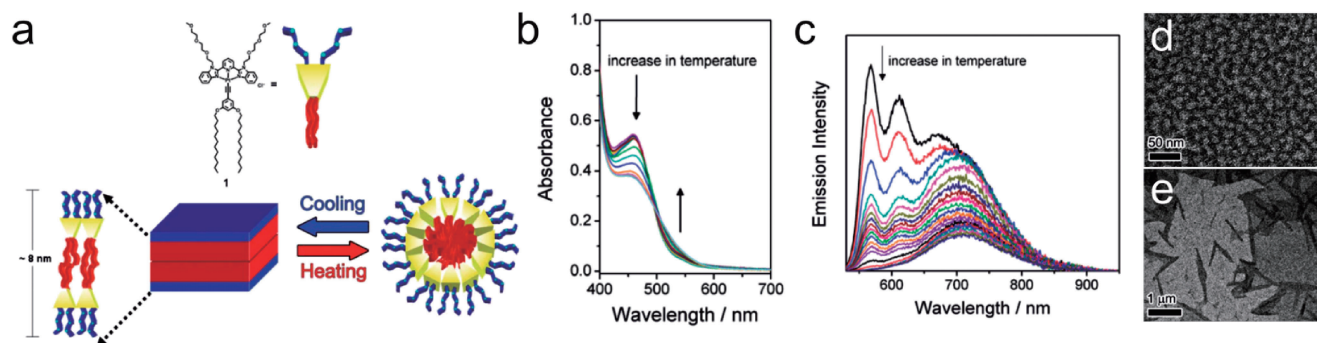
Figure 5. (a) Schematic diagram showing the formation of the bilayered sheet and micelle of compound **3**. Temperature-dependent UV–vis absorption (b) and emission spectra (c) obtained upon heating an aqueous solution of **3** ($c = 1 \times 10^{-4}$ M). Adapted from ref 49 with permission of The Royal Society of Chemistry.

Interestingly also polyhedral oligomeric silsesquioxane (POSS) moieties can be incorporated onto such class of Pt(II) complexes resulting in organosilane hybrids that still exhibit self-association behavior.[50] Importantly, various distinguishable nanostructures, associated with spectroscopic changes due the establishment of Pt···Pt and π–π interactions, can be formed in various solvent media ranging from nanorings to rods, opening up a new strategy for the development of new functional supramolecular materials with defined shape.

Another interesting approach to build up soft nanomaterials with phosphorescent organoplatinum(II) complexes consists of combining metallophilicity with ionic self-assembly. A nice example has been very recently reported by Chen et al.[51] in which cationic Pt(II) derivatives are rendered soluble in nonpolar solvents by counter ion metathesis with a highly lipophilic anion (complex **4** in Chart 1). Although such compounds are also soluble in polar solvents, the spectroscopic features observed in nonpolar solvents are distinct from those in the formers and the bathochromic shifted absorption/emission spectra have been used to discern monomeric to oligomeric

species. Interestingly, complex **4** can be engineered into honeycomb mesostructures by drop-casting a dilute (0.5 wt %) CH$_2$Cl$_2$ solution onto a SiO$_2$ wafer. SEM micrographs of the so-prepared film showed honeycomb patterns assembled presumably through extended metallophilic interactions and ionic self-assembly and covering an area of tens of mm^2, where each edge of the hexagons is about 1 µm long and 200 nm wide (Figure 6).

Incorporation of chiral moieties onto the molecular structures can lead to the formation of chiral supramolecular architectures such as helicoidal fibers[52,53] and metallogels.[54] In this respect, a recent example of the formation of chiral supramolecular structures has been reported by Yi and co-workers[55] who have synthesized a series of amphiphilic bipyridyl alkynylplatinum(II) complexes bearing cholesteric groups and ethylene glycol chains (complex **5** in Chart 1). Although all the three reported complexes can self-assemble forming gel networks, only the derivative without ether chains displayed well-defined right-handed helical structures (Figure 7). Nonetheless, compound **5** showed an interesting solvent-dependent chiral switching of self-assembled structure, where
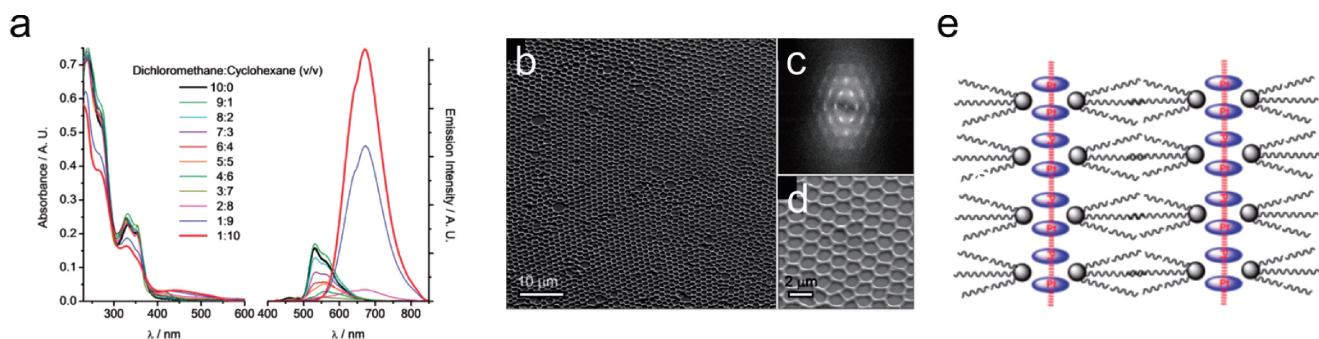
Figure 6. (a) UV–vis absorption and emission ($\lambda_{ex} = 378\,nm$) traces at 298 K for **4** in dichloromethane/cyclohexane mixtures upon increasing the cyclohexane percentage from 0 to 100% ($c = 2.0 \times 10^{-5}\,mol\,dm^{-3}$); b) SEM micrograph and its corresponding fast Fourier transform image (c) of the honeycomb mesostructured formed by **4** onto the surface of a silicon wafer; d) zoom-in SEM micrograph; e) proposed molecular packing. Adapted from ref 51 with permission of The Royal Society of Chemistry.
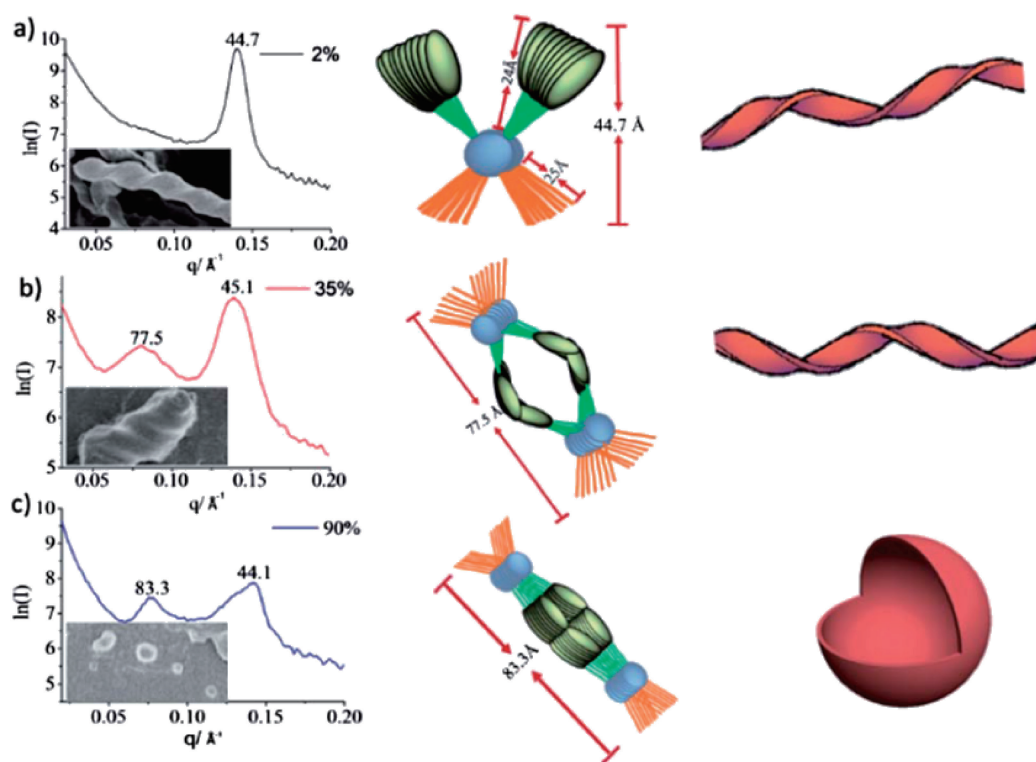
Figure 7. Correlation of the SAXS pattern, SEM image and packing model of **5** in ethanol upon increasing the water content to 2% (a), 35% (b), and 90% (c). Adapted from ref 55 with permission of The Royal Society of Chemistry.

the longer ethylene glycol chains forms regular left-handed helical structures in aqueous EtOH solution at H$_2$O content <5% v/v. As H$_2$O ratio increased, the chirality changed from left- to right-handed helix as supported by CD spectroscopy, with concomitant alteration of the packing mode from monolayer to hexagonal motifs. At water content greater than 50% v/v, the structure finally transforms into bilayer vesicles with loss of CD signal (Figure 7). The observed morphological changes were ascribed as due to a delicate balance between hydrophobic and hydrophilic interactions.

Another example of supramolecular self-assembly of chiral structures has been reported by Yam and co-workers[56] who have

shown how achiral alkynylplatinum(II) complexes can interact with carboxylic β-1,3-glucan motifs leading to chiral helicoidal structures (complex **6** in Chart 1). Interestingly, the handedness of this two-component helical assembly is affected by different parameters such as temperature, aging, components ratios, and mode of preparation and was tentatively rationalized in terms of kinetic vs. thermodynamic control.

Moreover, when chiral moieties are incorporated onto luminescent Pt(II) complexes, the self-assembly process can lead to chiral supramolecular architectures that nicely display circularly polarized luminescence. An interesting example has been very recently reported by Zhang et al.[57] who have
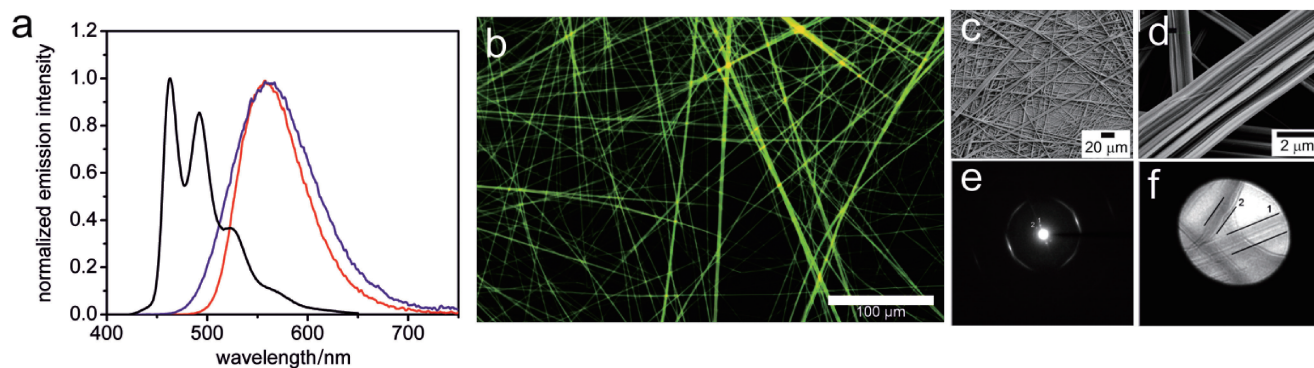
Figure 8. Emission spectra obtained for complex **8** (black trace) at a concentration of 5×10^{-5} M, self-assembled fibers obtained from acetone (red trace) and from CH_2Cl_2 (blue trace) at a concentration of $4\,mg\,mL^{-1}$ ($\lambda_{exc} = 300\,nm$); (b) fluorescence microscopy image of the fibers obtained from acetone ($\lambda_{exc} = 400–440\,nm$, scale bar: 100 mm). SEM images of fibers obtained from acetone (c) and a zoom-in image (d); SAED pattern (e) and the corresponding shadow image (f). Adapted from ref 58 with permission of The Royal Society of Chemistry.

synthesized chiral cyclometalated Pt(II) complexes by incorporating an enantiopure pinene group onto the chromophoric terdentate ligand (complex **7a** in Chart 1). Solvent-induced aggregation of such compound led to the formation of one-dimensional helical structures through Pt···Pt, π–π, and hydrophobic–hydrophobic interactions with enhanced and distinct chiroptical properties, which can be reversibly switched *on* and *off* upon temperature change.

Another important class of neutral platinum(II) complexes able to self-assemble into highly emissive species has been very recently reported by our group.[58,59] These derivatives contain dianionic $N_{trz}{}^{\wedge}N_{py}{}^{\wedge}N_{trz}$-based ligands as chromophoric moiety, where trz is a 1,2,4-triazolate moiety and py is a pyridyl group, and an ancillary pyridine which can be functionalized to improve solubility and tune self-assembly properties.

In this respect, Mauro et al.[58] have recently reported a neutral Pt(II) complex which bears CF_3 groups on the triazolyl moieties and an 4-amylpyridine as the ancillary ligand (complex **8** in Chart 1).

While such complex displayed a structured and weak (PLQY = 2%) blue emission upon photoexcitation; if an acetone solution of the complex is slowly concentrated by evaporation or aged, the complex molecules self-organize into discrete microcrystalline fibers which display intense (PLQY as high as 0.74) and featureless emission centered at $\lambda_{em} = 559\,nm$. As shown in Figure 8, electron microscopy analysis as well as small-angle X-ray scattering (SAXS) have shown that the emissive soft-structures prepared from acetone are comprised of hundreds of micrometer-long 1D fibers with high crystallinity, being probably the result of a self-assembly process of thinner nanostructures such as nanofibrils. The sizeable bathochromic shift and appearance of a lower energy band in the excitation spectrum are firm indications of the formation of ground state Pt···Pt interactions. Thus, the observed featureless emission was associated to an excited state with ^{3}MMLCT character. Noteworthy, the high directionality imparted by Pt···Pt and π–π stacking interaction to the assembled structures resulted in a linearly polarized emission upon fiber formation.

An attempt to control the formation of metallophilic interactions confined onto a 2D surface has been reported by

Bhowmick et al.[60] In their work, the authors reported on how $N_{trz}{}^{\wedge}N_{py}{}^{\wedge}N_{trz}$ platinum complexes could be assembled onto either amorphous quartz or 6H-SiC(0001) surfaces by wet chemical grafting. They found that upon coordination of the silane-grafted monodentate pyridine unit to the $N_{trz}{}^{\wedge}N_{py}{}^{\wedge}N_{trz}$-platinum moiety, resulting complexes are forced to aggregate as consequence of surface constraints, although bulky substituents such as adamantyl moieties are present.

Replacement of the 1,2,4-triazole moieties with isomeric 1,2,3-triazole ring leads to neutral tridentate 2,6-bis(1,2,3-triazol-4-yl)pyridine ligands and nicely allowed investigation of the role of the charge in the self-assembly properties by means of joint structural and photophysical techniques. A series of cationic Pt(II) complexes bearing monoanionic ancillary ligands (either Cl^- or CN^-) has been reported by De Cola and co-workers and are displayed in Figure 9.[61] They found that in such derivatives variation of the substitution pattern on either tridentate 1,2,3-triazole moieties and ancillary ligand affects the intermolecular interactions between neighbor complexes and, therefore, the degree of electronic overlap between the platinum centers. Interestingly, all the compounds possessing Cl^- as the ancillary ligand were not photoluminescent at room temperature and did not display any self-assembly property; while, the presence of more π-accepting ancillary ligand, such as CN^-, induces assembly upon establishment of Pt(II)···Pt(II) interactions and led to emissive Pt aggregates when bulky adamantyl groups were replaced with more planar phenyl moieties (Figure 9).

The replacement of 1,2,3-triazolyl moieties with 1,2,3,4-tetrazolyl rings leads to dianionic terdentate ligand that combined with a neutral ancillary moiety, such as substituted pyridines, results in neutral Pt(II) complexes with high stacking tendency toward formation of 1D fibrils. Such fibers often bundle into entangled 3D networks leading to the formation of highly emissive supramolecular gels as reported by Strassert et al.[62] In their recent communication, the authors have shown that while molecularly dissolved Pt(II)-tetrazole complex **9** (Chart 1) displayed no luminescence at room temperature; using the compound as low-molecular-weight gelating agent, a metallogel that can reach PLQY up to 90% can be prepared. They also
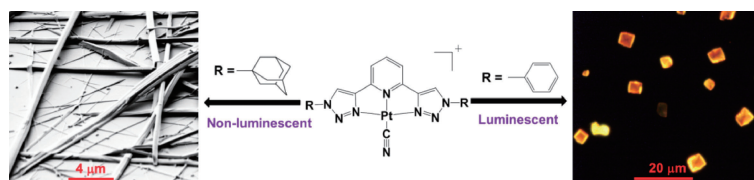
Figure 9. Schematic representation of the effects of the different functionalization of the triazole moieties on the luminescent and morphological properties of the resulting self-assembled structures. Adapted with permission from ref 61. Copyright (2015). American Chemical Society.
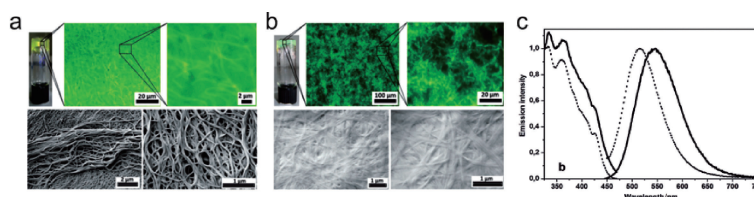
Figure 10. Fluorescence microscope images (top) and SEM images (bottom) of CH_2Cl_2 (a) and DMF (b) gels of complex **9**. (c) Excitation (left) and emission (right) spectra of the CH_2Cl_2 gel (solid line) and DMF gel (dotted line). Adapted from ref 63 with permission of The Royal Society of Chemistry.

demonstrated that gelation, morphological as well as photoluminescence properties of the resulting 3D network could be tuned by further functionalization of the ancillary pyridine. As an example, introduction of tetraethylene glycol chain[63] led to a reversible formation of highly luminescent gels in both CH_2Cl_2 and DMF with solvent-dependent photophysical properties and morphology (Figure 10).

The corresponding self-assembled fibers of complex **9** can be prepared by either pouring a CH_2Cl_2 solution of the complex into cyclohexane or drop-casting the CH_2Cl_2 solution directly onto a glass slide leading to bundled filaments. Furthermore, if the critical gelating concentration is reached, supramolecular metallogel formation takes place and the so-formed gel collapses into sol by shaking or sonication. In a different manner, the gel can be reversibly obtained upon thermal treatment when DMF is employed. Both gels were photoluminescent under UV light excitation, whereas the corresponding sols are not emissive in the same condition. The luminescence characteristic of the gel states was attributed as arising from and excited state with ^{3}MMLCT and displayed intense broad emission maximum centered at $\lambda_{em} = 550$ and $515\,nm$ for CH_2Cl_2 and DMF (PLQY = 60%) as solvent, respectively. SEM and fluorescence microscopy images of xerogel and gel, respectively, showed that the latter is constituted by a dense entanglement of fibers leading to a 3D network. The different PLQY value recorded for the gel prepared from CH_2Cl_2 and DMF was attributed to the different solvation of the polar PEG tail and the apolar chromophoric part in the two solvents. Indeed, the Pt(II) center is expected to interact more strongly with the apolar CH_2Cl_2, whereas the polar chains entangle in order to reduce their exposure to the solvent, thus bundling on the same side. On the other hand, in DMF, the Pt⋯Pt interactions are less pronounced due to the solvation of the polar PEG chains, thus preventing a closer approach of the metal centers. Consequently, the PEG chains could adopt an alternating configuration that favors a longer-range order and therefore increase emission quantum yield. The addition of a

second tetraethylene glycol chain to the ancillary pyridine increased further the amphiphilic character of the molecule allowing the preparation of phosphorescent hydrogels through host–guest interactions between cyclodextrins and the tetraethylene glycol tails of the Pt(II) complex.[64]

In summary, several classes of square-planar Pt(II) complexes were reported to yield highly luminescent supramolecular self-assembled structures. The proper design of the chelating ligands in terms of both bulkiness and electronic properties allows the formation of architectures with different morphologies, shapes and interesting functions as well as the modulation of the photophysical features. As hereafter discussed, these investigations paved the way for their use as active materials in different field of applications.

Mechanochromic Systems

Interest in stimuli-responsive materials has been largely increasing in the last decade, in the ongoing effort to develop artificial systems that can dynamically interact with their environment. The specific input and output of a responsive system, i.e. the stimulus and the material property subject to change, determine the field of application of the responsive material. Pt complexes have been found to change either (or both) absorption and emission colors as a result of a variety of stimuli, including vapors of volatile organic compounds (VOCs) as recently reviewed by Wenger[65] and Kato,[25] as well as mechanical stresses such as grinding, scraping, or compression.[66] Both absorption and emission colors are excellent signal candidates for sensing applications, since the sensitivity of human eye and of common charge-coupled device (CCD) sensors allows for implementation of fast tests performed by individual, nontrained persons, or by low-cost automated sensors such as smartphone or industrial cameras.

Nonetheless, luminescence overcomes absorption by several orders of magnitude in terms of sensitivity, and it is thus

compulsorily the signal of choice when miniaturization is required.

Following these considerations, we will focus this section on strongly emitting Pt complexes whose luminescence responds to mechanical stresses. Their responsiveness can lead to application of these materials in important fields such as sensing, security, and data storage.[66]

The particular interest on Pt(II) complexes as mechanochromic materials arises from the peculiar tunability of their luminescence spectrum as a function of metal⋯metal distance. In particular, spectral variations can be schematized as two-steps transitions, occurring when shortening the distance between two adjacent Pt complexes. First, a very sharp transition takes place when Pt⋯Pt distance becomes shorter than approximately 3.5 Å: metal–metal interaction triggers energy levels splitting and formation of a new ^{3}MMLCT band. This MO diagram change results in a correspondingly sharp variation in emission spectra, where a structured band corresponding to ^{3}MLCT transition disappears and a broader, unstructured band appears. The latter is typically bathochromically-shifted by a degree of 70–200 nm and can be ascribed to an excited state with ^{3}MMLCT character. This constitutes a truly efficient switch with both *ON–OFF* and *OFF–ON* signals to be monitored, which, combined together, yield a strong ratiometric signal in the visible range, i.e. a color change detectable by human eye or by CCD camera without the need for lengthy calibration procedures. Secondly, a smoother transition can occur when the Pt⋯Pt distance is tuned below 3.5 Å: in this case, a continuous bathochromic shift of the emission band can be observed, which provides *i)* deeper insight on the aggregation state; *ii)* allows to differentiate aggregates with different Pt⋯Pt distances; *iii)* allows design of multiple states (multiplexing) optoelectronic devices.

In the following paragraphs we will review the most recent investigations showing powerful examples of mechanochromic Pt complexes exhibiting both sharp spectral transitions and fine-tuning of the peak wavelength of the ^{3}MMLCT luminescence band.

In a recent contribution,[67] Ni and co-workers were able to prepare a diimine-platinum(II) complex, 10, with 4-bromo-2,2′-bipyridine, (Chart 2), that exhibits mechanoresponsive luminescence, with the typical spectral transition from a structured band to unstructured broad emission, and corresponding shift in peak emission wavelength of 165 nm upon grinding. X-ray diffraction studies (XRD) revealed that such spectral variation corresponds to a crystalline-to-amorphous state transition. Interestingly, an analogous crystalline-to-amorphous transition was observed upon heating the Pt complex, apart from the fact that the broad emission band was in this case shifted by only about 100 nm. This result suggests that the final amorphous aggregation state, and in particular the metal-to-metal distance, can strongly depend on the way energy is delivered to the Pt complex crystals. Mechanical grinding is hence able to bring metals closer, compared to heating. Remarkably, the heated amorphous aggregate can still be transformed into the ground aggregate upon thorough grinding, proving that the deeply red-shifted emission state can be obtained not only starting from the crystalline structure but also from other amorphous aggregates with larger Pt⋯Pt distances.

The same researchers found that the final emission wavelength of the broad band corresponding to the ground aggregates
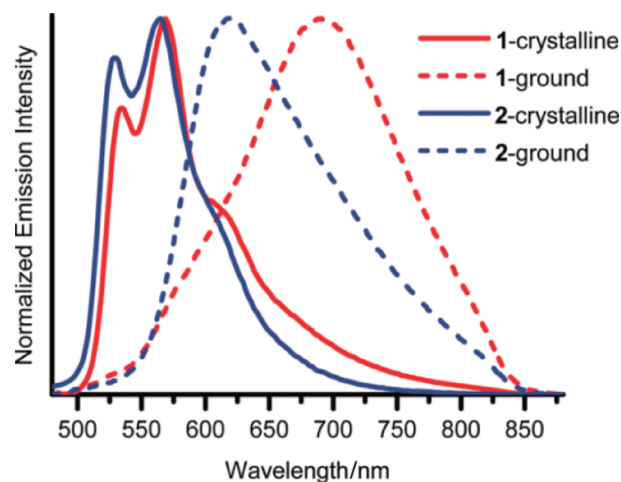
Figure 11. An example of solid-state Pt(II) complex emission in absence of metallophilic interactions (solid traces), and in presence of metallophilic interactions after grinding, with longer (blue dashed trace) or shorter (red dashed trace) Pt⋯Pt distance as determined by the bulkiness of the ligands in complex 11 and in its counterpart without *tert*-butyl pendants. Adapted with permission from ref 68. Copyright (2011). American Chemical Society.

can be tuned with the bulkiness of ligand substitutions (Figure 11).[68]

They ascribe the much smaller bathochromic shift of a *tert*-butyl-substituted derivative, complex 11 in Chart 2, −89 nm vs. 155 nm, the latter observed in absence of *tert*-butyl pendant to the longer Pt⋯Pt distance induced by the hindrance of this bulky lateral group. The effect of spatially encumbered ligands was also explored by Tsai and co-workers. Similarly, they concluded that bulky substituents favor the formation of monomer-like emitting crystals, which can then show mechanoresponsive properties if the substituents allow the crystalline structure to have enough sliding freedom (complex 12 in Chart 2).[69]

A more recent paper reports the synthesis of a series of imidoylamidinato platinum(II) complexes featuring bright luminescence in solid state and mechanochromic behavior.[70]

Even though the ground state of Pt complexes has always been found to be an amorphous aggregate state, Eisenberg and co-workers were able to record X-ray structures of a red-emitting polymorph of a terpyridyl Pt complex, 13 (Chart 2), analogous to the red-emitting ground aggregate. Their findings allowed them to conclude that mechanical stresses induce slipping of layers in the crystalline structure, resulting in a less dense aggregation state featuring Pt⋯Pt distances shorter than 3.5 Å.[71]

Remarkably, not all reports on mechanoresponsive Pt(II) complex agree that red-shifted emission arise from the formation of aggregates where strong metallophilic interactions take place as consequence of the establishment of short Pt⋯Pt distances. Early studies reported that the red-shifted emission of Pt(5dpb)Cl, 14 in Chart 2, where 5dpbH is 1,3-di(5-methyl-2-pyridyl)benzene, was the result of an interaction only taking place at the excited state, i.e. an excimer emission, as observed by time-resolved spectroscopy.[72]

Very recently, Swager and co-workers prepared a series of cationic cyclometalated Pt(II) complexes which form columnar
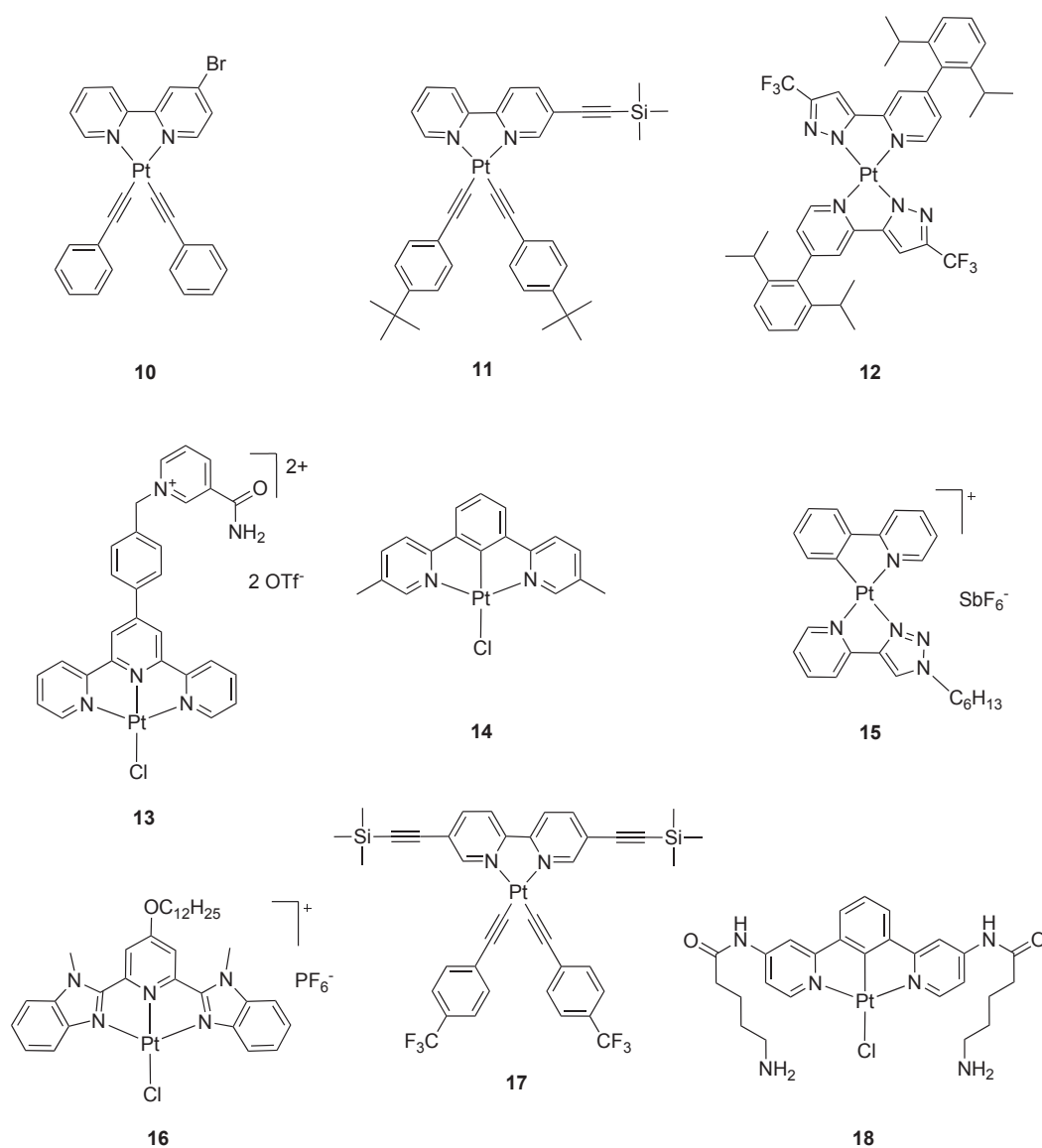
Chart 2. Chemical structures of the luminescent platinum(II) complexes displaying mechanochromic behavior and herein reviewed.

liquid crystal phases owing to the Pt⋯Pt interactions, acting as the dominant attractive force (Figure 12).[73]

Interestingly, their complex **15** (Chart 2) did not display emission properties in the liquid crystalline state in which the observed Pt⋯Pt distance ($d = 3.65$ Å) is at the threshold to trigger formation of ^{3}MMLCT band. Whereas the solid-state crystals showed a broad intense (PLQY up to 86%) luminescence band and exhibited mechanochromism as demonstrated by the bathochromic shift upon grinding. This was not the first report of Pt complexes forming liquid phase crystals responsive to tribological stimulation.[74] Furthermore, complex **15** showed strong dependence on environmental factors such as nature of polymer matrix in which it is embedded and doping level. Indeed, a bathochromic shift in the emission maximum was observed upon varying the polymer matrix, suggesting the possibility of tuning of the Pt⋯Pt distance in aggregated phases (Figure 13).

Embedment in polymer matrix is a key step for application of Pt complexes as responsive materials, in particular as sensors for pressure or mechanical stresses, or as memories. Methacrylate polymers have been identified as good candidates to obtain mechanically stable, responsive films. In addition, the possibility of changing the glass transition of the polymer matrix (T_g) with the length of the methacrylate chain allowed to investigate the role of T_g in the response of the luminescent Pt complexes embedded in polymers.[75]

It was found that mechanical as well as vapochromic response of complex **16** (Chart 2) was detectable and stable for high T_g polymers (poly(methyl methacrylate), $T_g = 90$ °C), while the same response was only temporary when T_g approached room temperature (poly(butyl methacrylate), $T_g = 30$ °C), as shown in Figure 14. Furthermore, as soon as each polymer mixture was heated above its T_g, the luminescence could be reset to the initial—non ground—state, while attempts
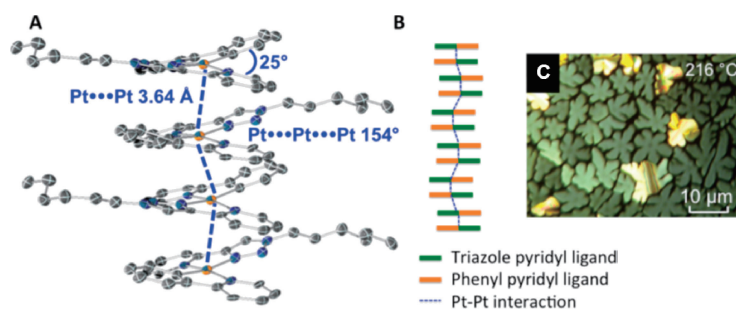
Figure 12. Mechanochromic Pt(II) complex forming columnar liquid crystals driven from Pt⋯Pt interactions. Crystal structure (A) and representation of stacking orientation (B) of the Col_h phase of complex **15** with BF_4^- counter ion, and (C) polarized optical micrograph of the Col_h phase of complex **15**. Adapted with permission from ref 73. Copyright (2014). American Chemical Society.
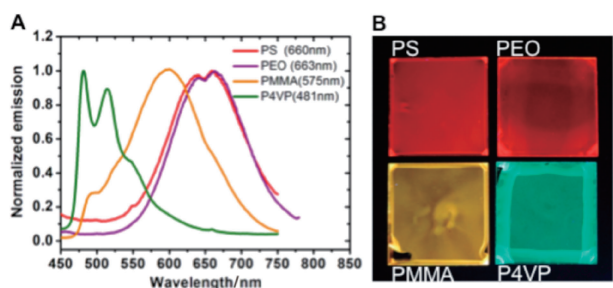
Figure 13. Emission spectra (A) and digital photograph under UV irradiation at 365 nm (B) of complex **15** embedded in different polymer matrixes, namely polystyrene (PS, red trace), poly(ethylene oxide) (PEO, magenta trace), poly(methyl methacrylate) (PMMA, orange trace) and poly(4-vinylpyridine) (green trace). Adapted with permission from ref 73. Copyright (2014). American Chemical Society.
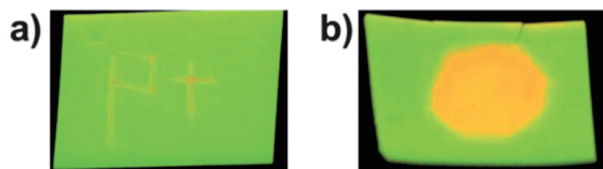
Figure 14. Mechanoluminescence response of a 10 wt % complex **16** in PMMA film observed under UV light ($\lambda_{exc} = 365$ nm) upon scratching (a) and after being hit sharply with a ball-peen hammer (b). Adapted from ref 75 with permission of The Royal Society of Chemistry.

to stress the films above T_g gave no observable response, due to the tendency of the polymer to flow, and thus to absorb the mechanical energy conveyed for structural rearrangement of the Pt(II) complex crystals.

PMMA was also employed by Chen and co-workers to obtain a device acting as a logic gate with mechanical and vapor based stimuli.[76] By using platinum complexes, bearing 4-trifluoromethylacetylide ligands, such as **17** in Chart 2, they were able to fabricate a proof-of-principle device that can be considered as an example of multistate logic gate (Figure 15). The device relies on the ability of Pt complexes to undergo not only the transition from absence to presence of metallophilic interactions, but also other transitions among structures showing different Pt⋯Pt distances. In their system, such different and well-defined Pt⋯Pt distances were induced by the inclusion of different volatile organic molecules in the crystal structure, while the ground powder exhibited the most red-shifted luminescence corresponding to an amorphous aggregate.

A similar phenomenon was observed by Kanbara and co-workers on complex **18** shown in Chart 2. The compound bears an amide moiety, which was responsible for setting different H-bond networks with DMF and MeOH, resulting in different Pt⋯Pt distances (emission maxima at 512 and 574 nm, respectively). Such metal distances could be further shortened upon grinding as demonstrated by the red shift of the emission peak of the ground aggregate down to 635 nm.[77]

An interesting development in terms of mechanoresponsive materials with optical reading was achieved by You and co-workers. They designed chiral Pt complex **7b** (Chart 1), which resulted responsive to mechanical stimuli. For such complex, not only the luminescence spectrum changes upon grinding, but even more interestingly the CD signal is completely depleted, which gives the opportunity to couple optical activity and luminescence color as the read-on signals.[78]

Finally, mechanoresponsiveness was also observed in Pt(II) heterometallic complexes,[79,80] while a recent review reports similar mechanoresponsive systems also based on other metals such as Au(I), Ag(I), Cu(I), and Ir(III).[81] Discussion of such derivatives is out of the scope of the present review.

Overall, the reversible and dynamic establishment of metallophilic interactions upon application of mechanical stimuli in platinum complexes as condensed phases represents a valuable and interesting manner to prepare luminescent stimuli-responsive materials with optical read-outs.

Optoelectronic Applications

Owing to the triplet nature of the emissive excited state and thus to the possibility to harvest both singlet and triplet electrogenerated excitons, luminescent Pt(II) complexes bearing either bidentate,[27] tridentate,[82,83] or tetradentate[84–86] coordination motifs have been extensively investigated as active materials in optoelectronic applications that include organic-light emitting diodes (OLEDs),[8] and organic light-emitting field-effect transitions (OLEFET).[33] To date, they represent the leading choice along with iridium-based counterparts. Nonetheless, contrarily to Ir(III) complexes which possess a d^6 electronic configuration
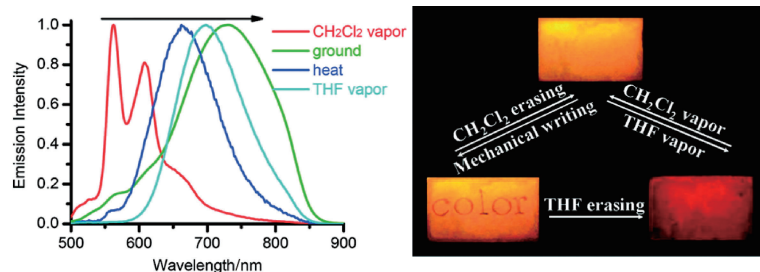
Figure 15. Solid-state emission spectra of complex **17** upon different stimuli (CH₂Cl₂ vapor, grinding, heat, and THF vapor, left) and the PMMA based device doped with complex **17** acting as a logic gate with mechanical and vapor based stimuli (right). Adapted with permission from ref 76. Copyright (2012). American Chemical Society.

and octahedral coordination geometry, Pt(II) complexes are able to display both ground and excited state aggregation through weak noncovalent bonds with π–π stacking, Pt···Pt interaction or both. Noteworthy, the spectral changes, such as bathochromic shift of the emission profile associated with the establishment of such interaction, allow the possibility to fabricate devices with improved features that include: *i*) better performance; *ii*) white-light emission,[69,87,88] when a single compound as emitter present as both monomeric and aggregated form is employed; *iii*) near infrared (NIR) emission,[89] and *iv*) charge-transport proprieties associated with the formation of extended Pt···Pt interactions.[33]

While broadening of the emission spectra as a consequence of intermolecular interactions could be ascribed to either ground or excited state aggregation, such interaction turns out to be often detrimental as it gives rise to species with poorer emission efficiencies and lower color purity, in particular for excimer emission.[90,91] We will thus hereafter refer to those cases in which the ground state aggregation yields to materials with improved performance in OLED devices.

In this respect, Williams, Roberto, and co-workers recently reported the use tridentate $N_{py}{}^\wedge C_{Ph}{}^\wedge N_{py}$ platinum derivatives, where N^C^N motifs is a substituted di(2-pyridyl)benzene bearing either Cl⁻ or NCS⁻ ancillary ligand (Chart 3).[89] The authors nicely demonstrated that, on one hand, both complexes displayed similar emission features in the fluid dilute solution with monomeric emission at λ_{em} of ca. 500 nm arising from a ³LC/³MLCT exited state. On the other hand, in the solid state complex **19-Cl** exhibited an excimer-like emission ($\lambda_{em} = 685$ nm), while the isothiocyanate derivative showed a sizeable bathochromic shift of 170 nm with a ³MMLCT emission squarely falling into the NIR region ($\lambda_{em} = 855$ nm), as consequence of the improved propensity towards aggregation through Pt···Pt and π–π interactions of the latter complex (Figure 16). Such unexpected behavior was also supported by X-ray structural determination analysis. Nicely, taking advantage of the establishment of such low-energy aggregate excited state, NIR-emitting OLED devices comprising neat film of complex **19-NCS**, as the active material, were fabricated which showed external quantum efficiency of 1% photons/electrons.

Upon changing the coordination motif from N^C^N to dianionic, tetrazolate-containing ligand (N^N^N), De Cola, Strassert, and co-workers were able to prepare a lipophilic neutral platinum complex **20** (Chart 3) bearing an ancillary *tert*-butylpyridine.[62] In this compound, the presence of the two tetrazolate moieties induces a sizeable stabilization of the
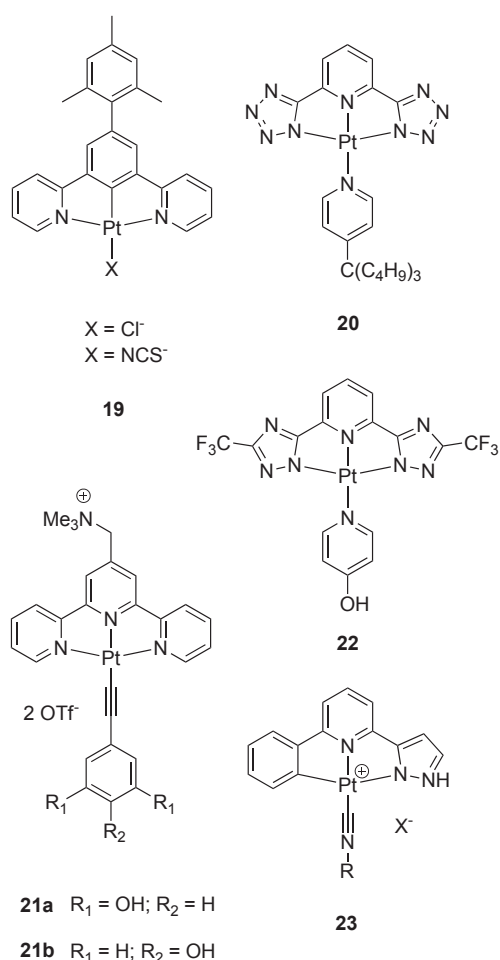
Chart 3. Chemical structures of the luminescent platinum(II) complexes used displaying aggregation through metallophilic interactions employed in light-emitting devices and bioimaging and herein reviewed.

highest occupied molecular orbital (HOMO) of the molecules with consequent increase of the lower-lying ³MLCT/³LC excited state which lies in energetic proximity to quenching state with either MC or LLCT nature. This is most likely the reason of the lack of emissive properties in solution for this complex as monomeric species. However, similarly to **9**,
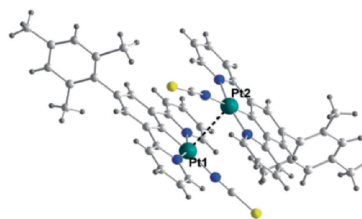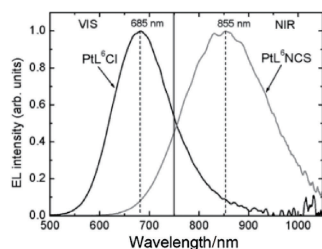
Figure 16. *Left*: electroluminescence spectra recorded for OLED employing neat film complex **19-Cl** and **19-NCS** as active layer. The diodes were biased at 14 V. *Right*: X-ray single-crystal structure of complex **19-NCS** displaying solid state Pt⋯Pt interaction ($d_{\text{Pt⋯Pt}}$ about 3.3 Å). Adapted from ref 89 with permission of The Royal Society of Chemistry.
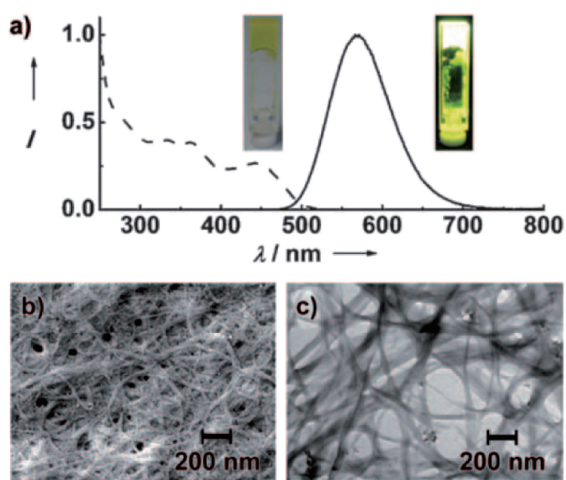
Figure 17. a) Excitation (dashed trace, $\lambda_{\text{exc}} = 420\,\text{nm}$) and emission (solid trace, $\lambda_{\text{em}} = 580\,\text{nm}$) spectra of the gel prepared from complex **20**. In the inset is displayed a photograph of the luminescent gel; b) SEM and c) TEM micrographs of the xerogel. Figure adapted from ref 62 with permission from Wiley.

complex **20** is capable of aggregating and gelling solvents yielding soft-materials with reduced triplet–triplet annihilation, PLQY of 90% and $\tau = 0.7\,\mu\text{s}$, and a bright yellow (λ_{em} ca. 570 nm) emission associated to a ^{3}MMLCT excited state upon complex aggregation via metallophilic and π–π interaction (Figure 17).

As demonstrated by SEM micrographs and optical confocal imaging, their material was characterized by highly phosphorescent entangled fibers containing the tetrazole-based platinum emitters, which were efficiently used as emissive component in solution-processed OLEDs. The so-fabricated light-emitting devices represented the first examples of OLEDs in which aggregates where directly used as active phosphorescent materials and displayed remarkable performance with peak current and power efficiency as high as 15.6 cd A^{-1} and 4.5 lm W^{-1} at 10 wt % doping level. Noteworthy, such performances are comparable with other solution-processed OLEDs employing monomeric Pt(II) emitters.[92–95]

In conclusion, it has been demonstrated that luminescent self-assembled structures can be used as active materials in optoelectronic application including OLEDs and OLEFETs. Taking advantage of the establishment of the Pt⋯Pt interaction,

novel and added-value features can be introduced such as NIR-emission and charge-transport properties; the latter as due to the anisotropic structural order imparted by such axial interaction.

Bioimaging Applications

Another field of application of luminescent transition-metal complexes, which is nowadays attracting growing interests, is their use for bioimaging purposes and several recent reviews have been dedicated to this topic.[15,16,96] Indeed, phosphorescent complexes possess different advantages when compared to organic luminophores such as reduced photobleaching, longer excited state lifetimes, large Stokes shift, sensitivity to the environment, such as pH, polarity, and rigidity. These characteristics make luminescent complexes suitable potential candidates for bioimaging labels and probes able to improve signal over background fluorescence ratio by using time gate techniques and lifetime-based imaging mapping.[97–99] However, they display severe drawbacks as *i*) triplet dioxygen quenching in air-equilibrated conditions, such as biological relevant environments, due to the formally triplet nature of their lowest-lying emitting excited state; *ii*) reduced tunability of the absorption and emission bands in the red and NIR region of the electromagnetic spectrum.[15] Even though several attempts have been made in order to shield the emitting excited states of such complexes from ^{3}O$_2$ quenching such as encapsulation in nanoparticles, dendrimeric systems, and soft matter structures (micelles, vesicles, etc.), tuning their photophysical properties deep into the visible and NIR, while keeping a relatively high PLQY, represents a major challenge.

Hence, the great tendency towards face-to-face stacking through ground state Pt⋯Pt and π–π interactions has been very recently explored as a powerful way to develop highly emitting bioimaging probes with great potentiality.[15] Indeed, the consequent formation of singlet- and triplet-manifold MMLCT bands in the excitation and emission spectra, respectively, induces a bathochromic shift of the both optical transitions with, in some cases, concomitant enhancement of PLQY.[100]

To this respect, Yam and co-workers reported on an series of water-dispersible σ-alkynyl Pt(II) complexes with phenolic ancillary moieties that squarely emit into the NIR region (derivatives **21a** and **21b** in Chart 3), yet with low PLQY.[101] Their derivatives displayed interesting pH-sensitive photophysical features in terms of both absorption and emission. Indeed, while at pH <5.6 (pK_a* = 6.27) complex **21a** showed a moderately intense emission centered λ_{em} ca. 800 nm arising

from a ^{3}MMLCT excited state of the aggregated complexes in such aqueous condition; upon increasing the pH close to the physiological condition (pH 7.0–7.4), a complete quenching of the emission was detected as concomitant consequence of *i*) complexes disaggregation, due to the increased hydrophilicity of the deprotonated phenolate moieties; *ii*) photoinduced electron transfer process involving the more electron-rich phenolate moieties. Their complexes were used as pH-responsive NIR-emitting probes for live Madin–Darby canine kidney (MDCK) cells for imaging acidic cellular compartments, namely lyso-zomes, under physiological temperature and pH by means of confocal microscopy.

Taking advantage of the spontaneous tendency towards aggregation through Pt···Pt interactions in neutral derivatives with pyridil-*bis*-CF$_3$-triazolyl chromophoric ligands, De Cola, Mauro, and co-workers demonstrated the use of such derivatives for bioimaging purposes (Figure 18).[102] In their paper, they were able to show that complex **22** (Chart 3) is readily internalized in living human cervical carcinoma (HeLa) cells and mostly accumulated into the nuclear region, as demonstrated by *z*-stack confocal microscopy and colocalization studies. Upon internalization, complex aggregation via establishment of metallophilic interactions induced a sizeable bathochromic shift of both absorption and emission MMLCT bands, which were efficiently used to shift the excitation wavelength down to $\lambda_{\text{exc}} = 543$ nm (low-lying ^{1}MMLCT band), an unprecedented result for non-porphyrinic phosphorescent bioprobes (Figure 18). In a similar manner, the internalized Pt(II) complexes showed a strong (PLQY = 36% in air-equilibrated DMSO:H$_2$O 1:99) long-lived emission centered at ca. 590 nm arising from a ^{3}MMLCT excited state. Furthermore, aggregation of the internalized complexes possesses multifold advantages when compared to nonaggregated derivatives. Indeed, aggregation might account for a physical shielding effect for the emitting excited state towards bimolecular dioxygen quenching and other biomolecules.

Finally, in more recent work Che and co-workers reported the use of cationic C$_{\text{phenyl}}^{N}_{\text{pyridine}}^{N}_{\text{pyrazole}}$ platinum complexes as pH-responsive luminescent bioimaging agents, with general

formula **23** as shown in Chart 3.[103] Their strategy stems from the ability of this class of emitting Pt derivative to establish intermolecular Pt···Pt and π–π interaction as a consequence of the presence of the pH-sensitive N–H moiety on the coordinated pyrazole unit.[104] Varying the substituent on the ancillary isocyanide group, the assembly–disassembly behavior via metallophophilic interaction upon pH modification was used, on one hand, for the formation of supramolecular hydrogel with bathochromically shifted ^{3}MMLCT emission and controlled release of cytotoxic complexes; on the other hand, for the selective imaging of lysosomes using aggregated red-emitting species predominant at such low physiological pH (pH ca. 5).

Finally, while organic fluorophores still represent the leading choice for application in bioimaging due to the possibility to easily tune both absorption and emission maxima; the use of phosphorescent platinum complexes has been demonstrate to display several advantages in terms of long-lived excited state lifetime as well as the peculiar possibility to shift both excitation and photoluminescence into the visible spectrum through establishment of metal···metal interactions into living cells. This approach might constitute a novel and powerful strategy towards the preparation of efficient phosphorescent biolabels.

Concluding Remarks

Supramolecular weak interactions can be efficiently used as powerful technique for preparing complex systems that display a variety of functions. In this view, the preparation of supra-molecular functional architectures with well-defined shape, size, and properties is of paramount importance towards the fabrication of performing devices and machineries by using *bottom-up* approaches, but it requires deep and comprehensive understanding of the supramolecular mechanisms and processes at play. In particular, the establishment of weak metallophilic and π–π interactions between neighbor platinum(II) complexes has been proven to induce profound changes to the properties, including redox, spectroscopic, and charge transport, in the assembled complexes as consequence of the d$_{z^2}$ orbitals axial interaction. In this Highlight Review, the most recent advances in such fascinating and very attractive field of research are presented. The selected examples discussed herein yield supra-molecular luminescent architectures from quasi-0D systems to 1D arrays, to 2D layers, and up to 3D networks. Furthermore, some appealing highlights are presented on attractive and innovative applications of such assembled systems for the preparation of mechanochromic materials as well as used as active components for optoelectronic devices and novel bio-imaging agents.
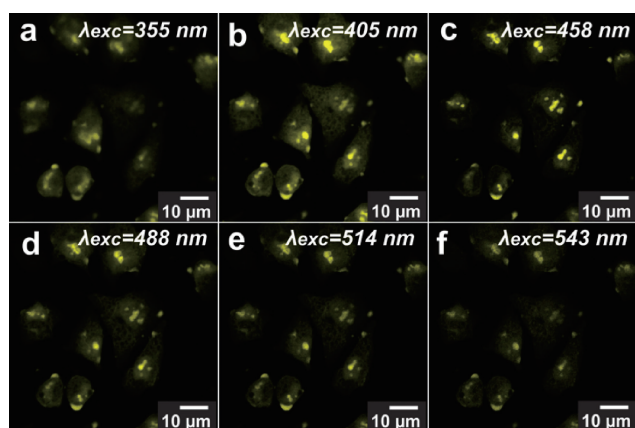
Figure 18. Fluorescence confocal microscopy images of HeLa cells stained with complex **22**, after 4 h incubation in PBS. The samples were excited at 355 (a), 405 (b), 458 (c), 488 (d), 514 (e), and 543 nm (f). Adapted from ref 102 with permission of The Royal Society of Chemistry.

References

1 *Photochemistry and Photophysics of Coordination Compounds I*, ed. by V. Balzani, S. Campagna, Springer Berlin Heidelberg, **2007**. doi:10.1007/978-3-540-73347-8.

2 A. Barbieri, G. Accorsi, N. Armaroli, *Chem. Commun.* **2008**, 2185.

3 Y. Hasegawa, T. Nakagawa, T. Kawai, *Coord. Chem. Rev.* **2010**, *254*, 2643.

4 R. Visbal, M. C. Gimeno, *Chem. Soc. Rev.* **2014**, *43*, 3551.

5 D. V. Scaltrito, D. W. Thompson, J. A. O'Callaghan, G. J. Meyer, *Coord. Chem. Rev.* **2000**, *208*, 243.

6 M. Panigati, M. Mauro, D. Donghi, P. Mercandelli, P. Mussini, L. De Cola, G. D'Alfonso, *Coord. Chem. Rev.* **2012**, *256*, 1621.

7 C. A. Strassert, M. Mauro, L. De Cola, in *Inorganic Photochemistry* in *Advances in Inorganic Chemistry*, ed. by R. van Eldik, G. Stochel, Elsevier Inc., Academic Press, **2011**, Vol. 63, pp. 47–103. doi:10.1016/B978-0-12-385904-4.00009-3.

8 *Highly Efficient OLEDs with Phosphorescent Materials*, ed. by H. Yersin, Wiley-VCH Verlag GmbH & Co. KGaA, **2008**. doi:10.1002/9783527621309.

9 R. D. Costa, E. Ortí, H. J. Bolink, F. Monti, G. Accorsi, N. Armaroli, *Angew. Chem., Int. Ed.* **2012**, *51*, 8178.

10 K. M.-C. Wong, M. M.-Y. Chan, V. W.-W. Yam, *Adv. Mater.* **2014**, *26*, 5558.

11 B. E. Hardin, H. J. Snaith, M. D. McGehee, *Nat. Photonics* **2012**, *6*, 162.

12 S. Mathew, A. Yella, P. Gao, R. Humphry-Baker, B. F. E. Curchod, N. Ashari-Astani, I. Tavernelli, U. Rothlisberger, M. K. Nazeeruddin, M. Grätzel, *Nat. Chem.* **2014**, *6*, 242.

13 A. Ruggi, F. W. B. van Leeuwen, A. H. Velders, *Coord. Chem. Rev.* **2011**, *255*, 2542.

14 V. Fernández-Moreira, F. L. Thorp-Greenwood, A. J. Amoroso, J. Cable, J. B. Court, V. Gray, A. J. Hayes, R. L. Jenkins, B. M. Kariuki, D. Lloyd, C. O. Millet, C. F. Williams, M. P. Coogan, *Org. Biomol. Chem.* **2010**, *8*, 3888.

15 M. Mauro, A. Aliprandi, D. Septiadi, N. S. Kehr, L. De Cola, *Chem. Soc. Rev.* **2014**, *43*, 4144.

16 Q. Zhao, C. Huang, F. Li, *Chem. Soc. Rev.* **2011**, *40*, 2508.

17 M. S. Lowry, J. I. Goldsmith, J. D. Slinker, R. Rohl, R. A. Pascal, Jr., G. G. Malliaras, S. Bernhard, *Chem. Mater.* **2005**, *17*, 5712.

18 M.-C. Tang, D. P.-K. Tsang, M. M.-Y. Chan, K. M.-C. Wong, V. W.-W. Yam, *Angew. Chem., Int. Ed.* **2013**, *52*, 446.

19 W.-P. To, K. T. Chan, G. S. M. Tong, C. Ma, W.-M. Kwok, X. Guan, K.-H. Low, C.-M. Che, *Angew. Chem., Int. Ed.* **2013**, *52*, 6648.

20 S. Bestgen, M. T. Gamer, S. Lebedkin, M. M. Kappes, P. W. Roesky, *Chem.—Eur. J.* **2015**, *21*, 601.

21 Y. Chen, G. Cheng, K. Li, D. P. Shelar, W. Lu, C.-M. Che, *Chem. Sci.* **2014**, *5*, 1348.

22 J. Muñiz, C. Wang, P. Pyykkö, *Chem.—Eur. J.* **2011**, *17*, 368.

23 D. Kim, J.-L. Brédas, *J. Am. Chem. Soc.* **2009**, *131*, 11371.

24 L. H. Doerrer, *Dalton Trans.* **2010**, *39*, 3543.

25 A. Kobayashi, M. Kato, *Eur. J. Inorg. Chem.* **2014**, 4469.

26 V. H. Houlding, V. M. Miskowski, *Coord. Chem. Rev.* **1991**, *111*, 145.

27 J. A. G. Williams, in *Photochemistry and Photophysics of Coordination Compounds II* in *Topics in Current Chemistry*, Springer, **2007**, Vol. 281, p. 205. doi:10.1007/128_2007_134.

28 J.-M. Lehn, *Supramolecular Chemistry: Concepts and Perspectives*, VCH, Weinheim, **1995**. doi:10.1002/3527607439.

29 J.-M. Lehn, *Angew. Chem., Int. Ed.* **2015**, *54*, 3276.

30 C. Yu, K. H.-Y. Chan, K. M.-C. Wong, V. W.-W. Yam, *Proc. Natl. Acad. Sci. U.S.A.* **2006**, *103*, 19652.

31 J. Moussa, K. M.-C. Wong, L.-M. Chamoreau, H. Amouri, V. W.-W. Yam, *Dalton Trans.* **2007**, 3526.

32 T. Cardolaccia, Y. Li, K. S. Schanze, *J. Am. Chem. Soc.* **2008**, *130*, 2535.

33 M.-Y. Yuen, V. A. L. Roy, W. Lu, S. C. F. Kui, G. S. M. Tong, M.-H. So, S. S.-Y. Chui, M. Muccini, J. Q. Ning, S. J. Xu, C.-M. Che, *Angew. Chem., Int. Ed.* **2008**, *47*, 9895.

34 W. Lu, Y. Chen, V. A. L. Roy, S. S.-Y. Chui, C.-M. Che, *Angew. Chem., Int. Ed.* **2009**, *48*, 7621.

35 W. Lu, S. S.-Y. Chui, K.-M. Ng, C.-M. Che, *Angew. Chem., Int. Ed.* **2008**, *47*, 4568.

36 Y. Guo, L. Xu, H. Liu, Y. Li, C.-M. Che, Y. Li, *Adv. Mater.* **2015**, *27*, 985.

37 Y.-J. Tian, E. W. Meijer, F. Wang, *Chem. Commun.* **2013**, *49*, 9197.

38 A. Aliprandi, M. Mauro, L. De Cola, submitted.

39 A. Y.-Y. Tam, K. M.-C. Wong, V. W.-W. Yam, *J. Am. Chem. Soc.* **2009**, *131*, 6253.

40 V. W.-W. Yam, Y. Hu, K. H.-Y. Chan, C. Y.-S. Chung, *Chem. Commun.* **2009**, 6216.

41 F. Camerel, R. Ziessel, B. Donnio, C. Bourgogne, D. Guillon, M. Schmutz, C. Iacovita, J.-P. Bucher, *Angew. Chem.* **2007**, *46*, 2659.

42 M. Chen, C. Wei, X. Wu, M. Khan, N. Huang, G. Zhang, L. Li, *Chem.—Eur. J.* **2015**, *21*, 4213.

43 K. M.-C. Wong, V. W.-W. Yam, *Acc. Chem. Res.* **2011**, *44*, 424.

44 K. H.-Y. Chan, J. W.-Y. Lam, K. M.-C. Wong, B.-Z. Tang, V. W.-W. Yam, *Chem.—Eur. J.* **2009**, *15*, 2328.

45 C. Yu, K. H.-Y. Chan, K. M.-C. Wong, V. W.-W. Yam, *Chem.—Eur. J.* **2008**, *14*, 4577.

46 C. Y.-S. Chung, V. W.-W. Yam, *Chem.—Eur. J.* **2014**, *20*, 13016.

47 C. Po, A. Y.-Y. Tam, K. M.-C. Wong, V. W.-W. Yam, *J. Am. Chem. Soc.* **2011**, *133*, 12136.

48 C. Po, A. Y.-Y. Tam, V. W.-W. Yam, *Chem. Sci.* **2014**, *5*, 2688.

49 C. Po, V. W.-W. Yam, *Chem. Sci.* **2014**, *5*, 4868.

50 H.-L. Au-Yeung, S. Y.-L. Leung, A. Y.-Y. Tam, V. W.-W. Yam, *J. Am. Chem. Soc.* **2014**, *136*, 17910.

51 Y. Chen, C.-M. Che, W. Lu, *Chem. Commun.* **2015**, *51*, 5371.

52 S. Y.-L. Leung, V. W.-W. Yam, *Chem. Sci.* **2013**, *4*, 4228.

53 S. Y.-L. Leung, W. H. Lam, V. W.-W. Yam, *Proc. Natl. Acad. Sci. U.S.A.* **2013**, *110*, 7986.

54 C. Po, Z. Ke, A. Y.-Y. Tam, H.-F. Chow, V. W.-W. Yam, *Chem.—Eur. J.* **2013**, *19*, 15735.

55 Y. Mao, K. Liu, L. Meng, L. Chen, L. Chen, T. Yi, *Soft Matter* **2014**, *10*, 7615.

56 C. Y.-S. Chung, S. Tamaru, S. Shinkai, V. W.-W. Yam, *Chem.—Eur. J.* **2015**, *21*, 5447.

57 X.-P. Zhang, V. Y. Chang, J. Liu, X.-L. Yang, W. Huang, Y. Li, C.-H. Li, G. Muller, X.-Z. You, *Inorg. Chem.* **2015**, *54*, 143.

58 M. Mauro, A. Aliprandi, C. Cebrián, D. Wang, C. Kübel, L. De Cola, *Chem. Commun.* **2014**, *50*, 7269.

59 M. Mydlak, M. Mauro, F. Polo, M. Felicetti, J. Leonhardt, G. Diener, L. De Cola, C. A. Strassert, *Chem. Mater.* **2011**, *23*, 3659.

60 D. K. Bhowmick, L. Stegemann, M. Bartsch, N. K. Allampally, C. A. Strassert, H. Zacharias, *J. Phys. Chem. C* **2015**, *119*, 5551.

61 N. K. Allampally, C.-G. Daniliuc, C. A. Strassert, L. De Cola, *Inorg. Chem.* **2015**, *54*, 1588.

62 C. A. Strassert, C.-H. Chien, M. D. Galvez Lopez, D. Kourkoulos, D. Hertel, K. Meerholz, L. De Cola, *Angew. Chem., Int. Ed.* **2011**, *50*, 946.

63 N. K. Allampally, C. A. Strassert, L. De Cola, *Dalton Trans.* **2012**, *41*, 13132.

64 N. K. Allampally, M. Bredol, C. A. Strassert, L. De Cola, *Chem.—Eur. J.* **2014**, *20*, 16863.

65 O. S. Wenger, *Chem. Rev.* **2013**, *113*, 3686.

66 Y. Sagara, T. Kato, *Nat. Chem.* **2009**, *1*, 605.

67 J. Ni, Y.-G. Wang, H.-H. Wang, L. Xu, Y.-Q. Zhao, Y.-Z. Pan, J.-J. Zhang, *Dalton Trans.* **2014**, *43*, 352.

68 J. Ni, X. Zhang, N. Qiu, Y.-H. Wu, L.-Y. Zhang, J. Zhang, Z.-N. Chen, *Inorg. Chem.* **2011**, *50*, 9090.

69 L.-M. Huang, G.-M. Tu, Y. Chi, W.-Y. Hung, Y.-C. Song, M.-R. Tseng, P.-T. Chou, G.-H. Lee, K.-T. Wong, S.-H. Cheng, W.-S. Tsai, *J. Mater. Chem. C* **2013**, *1*, 7582.

70 T. Tanaka, R. Nouchi, Y. Nakao, Y. Arikawa, K. Umakoshi, *RSC Adv.* **2014**, *4*, 62186.

71 A. Han, P. Du, Z. Sun, H. Wu, H. Jia, R. Zhang, Z. Liang, R. Cao, R. Eisenberg, *Inorg. Chem.* **2014**, *53*, 3338.

72 T. Abe, T. Itakura, N. Ikeda, K. Shinozaki, *Dalton Trans.* **2009**, 711.

73 M. Krikorian, S. Liu, T. M. Swager, *J. Am. Chem. Soc.* **2014**, *136*, 2952.

74 V. N. Kozhevnikov, B. Donnio, D. W. Bruce, *Angew. Chem., Int. Ed.* **2008**, *47*, 6286.

75 J. R. Kumpfer, S. D. Taylor, W. B. Connick, S. J. Rowan, *J. Mater. Chem.* **2012**, *22*, 14196.

76 X. Zhang, J.-Y. Wang, J. Ni, L.-Y. Zhang, Z.-N. Chen, *Inorg. Chem.* **2012**, *51*, 5569.

77 S. J. Choi, J. Kuwabara, Y. Nishimura, T. Arai, T. Kanbara, *Chem. Lett.* **2012**, *41*, 65.

78 X.-P. Zhang, J.-F. Mei, J.-C. Lai, C.-H. Li, X.-Z. You, *J. Mater. Chem. C* **2015**, *3*, 2350.

79 J. R. Berenguer, E. Lalinde, A. Martín, M. T. Moreno, S. Ruiz, S. Sánchez, H. R. Shahsavari, *Inorg. Chem.* **2014**, *53*, 8770.

80 T. Ohba, A. Kobayashi, H.-C. Chang, M. Kato, *Dalton Trans.* **2013**, *42*, 5514.

81 X. Zhang, Z. Chi, Y. Zhang, S. Liu, J. Xu, *J. Mater. Chem. C* **2013**, *1*, 3376.

82 J. A. G. Williams, A. Beeby, E. S. Davies, J. A. Weinstein, C. Wilson, *Inorg. Chem.* **2003**, *42*, 8609.

83 J. A. G. Williams, S. Develay, D. L. Rochester, L. Murphy, *Coord. Chem. Rev.* **2008**, *252*, 2596.

84 D. A. K. Vezzu, J. C. Deaton, J. S. Jones, L. Bartolotti, C. F. Harris, A. P. Marchetti, M. Kondakova, R. D. Pike, S. Huo, *Inorg. Chem.* **2010**, *49*, 5107.

85 G. Cheng, S. C. F. Kui, W.-H. Ang, M.-Y. Ko, P.-K. Chow, C.-L. Kwong, C.-C. Kwok, C. Ma, X. Guan, K.-H. Low, S.-J. Su, C.-M. Che, *Chem. Sci.* **2014**, *5*, 4819.

86 X.-C. Hang, T. Fleetham, E. Turner, J. Brooks, J. Li, *Angew. Chem., Int. Ed.* **2013**, *52*, 6753.

87 B. Ma, P. I. Djurovich, S. Garon, B. Alleyne, M. E. Thompson, *Adv. Funct. Mater.* **2006**, *16*, 2438.

88 W. Mróz, C. Botta, U. Giovanella, E. Rossi, A. Colombo, C. Dragonetti, D. Roberto, R. Ugo, A. Valore, J. A. G. Williams, *J. Mater. Chem.* **2011**, *21*, 8653.

89 E. Rossi, A. Colombo, C. Dragonetti, D. Roberto, F. Demartin, M. Cocchi, P. Brulatti, V. Fattori, J. A. G. Williams, *Chem. Commun.* **2012**, *48*, 3182.

90 E. Rossi, L. Murphy, P. L. Brothwood, A. Colombo, C. Dragonetti, D. Roberto, R. Ugo, M. Cocchi, J. A. G. Williams, *J. Mater. Chem.* **2011**, *21*, 15501.

91 E. Rossi, A. Colombo, C. Dragonetti, D. Roberto, R. Ugo, A. Valore, L. Falciola, P. Brulatti, M. Cocchi, J. A. G. Williams, *J. Mater. Chem.* **2012**, *22*, 10650.

92 C. Cebrián, M. Mauro, D. Kourkoulos, P. Mercandelli, D. Hertel, K. Meerholz, C. A. Strassert, L. De Cola, *Adv. Mater.* **2013**, *25*, 437.

93 G. Cheng, Y. Chen, C. Yang, W. Lu, C.-M. Che, *Chem.—Asian J.* **2013**, *8*, 1754.

94 M. Cocchi, D. Virgili, V. Fattori, D. L. Rochester, J. A. G. Williams, *Adv. Funct. Mater.* **2007**, *17*, 285.

95 C.-M. Che, C.-C. Kwok, S.-W. Lai, A. F. Rausch, W. J. Finkenzeller, N. Zhu, H. Yersin, *Chem.—Eur. J.* **2010**, *16*, 233.

96 E. Baggaley, J. A. Weinstein, J. A. G. Williams, *Coord. Chem. Rev.* **2012**, *256*, 1762.

97 S. W. Botchway, M. Charnley, J. W. Haycock, A. W. Parker, D. L. Rochester, J. A. Weinstein, J. A. G. Williams, *Proc. Natl. Acad. Sci. U.S.A.* **2008**, *105*, 16071.

98 E. Baggaley, S. W. Botchway, J. W. Haycock, H. Morris, I. V. Sazanovich, J. A. G. Williams, J. A. Weinstein, *Chem. Sci.* **2014**, *5*, 879.

99 E. Baggaley, I. V. Sazanovich, J. A. G. Williams, J. W. Haycock, S. W. Botchway, J. A. Weinstein, *RSC Adv.* **2014**, *4*, 35003.

100 R. Soldati, A. Aliprandi, M. Mauro, L. De Cola, D. Giacomini, *Eur. J. Org. Chem.* **2014**, 7113.

101 C. Y.-S. Chung, S. P.-Y. Li, M.-W. Louie, K. K.-W. Lo, V. W.-W. Yam, *Chem. Sci.* **2013**, *4*, 2453.

102 D. Septiadi, A. Aliprandi, M. Mauro, L. De Cola, *RSC Adv.* **2014**, *4*, 25709.

103 J. L.-L. Tsai, T. Zou, J. Liu, T. Chen, A. O.-Y. Chan, C. Yang, C.-N. Lok, C.-M. Che, *Chem. Sci.* **2015**, *6*, 3823.

104 C.-K. Koo, B. Lam, S.-K. Leung, M. H.-W. Lam, W.-Y. Wong, *J. Am. Chem. Soc.* **2006**, *128*, 16434.